

Pion Pressure in a Magnetic Field

Christoph P. Hofmann^a

^a Facultad de Ciencias, Universidad de Colima
Bernal Díaz del Castillo 340, Colima C.P. 28045, Mexico

January 23, 2022

Abstract

While the partition function for QCD in a magnetic field H has been calculated before within chiral perturbation theory up to two-loop order, our investigation relies on an alternative representation for the Bose functions which allows for a clear-cut expansion of thermodynamic quantities in the chiral limit. We first focus on the pion-pion interaction in the pressure and show that – depending on magnetic field strength, temperature and pion mass – it may be attractive or repulsive. We then analyze the thermodynamic properties in the chiral limit and provide explicit two-loop representations for the pressure in the weak magnetic field limit $|qH| \ll T^2$.

1 Introduction

The low-energy properties of quantum chromodynamics (QCD) can be understood on the basis of its relevant low-energy degrees of freedom: the Goldstone bosons. This is the path pursued by chiral perturbation theory (CHPT) and indeed, the low-temperature properties of QCD in a magnetic field have been explored within CHPT in many studies up to two-loop order [1–12]. Other approaches to finite temperature QCD in magnetic fields include lattice QCD [13–25], Nambu-Jona-Lasinio model-based studies [26–33], and other techniques [34–60]. Yet more references can be found in the review Ref. [61].

Recently, the present author has pointed out that the low-temperature expansion of the quark condensate in a weak magnetic field and in the chiral limit has not been

properly derived, and has provided the correct series in Ref. [62]. The analysis was based on an alternative representation for the Bose functions which was the key to derive the proper series in a transparent manner. Relying on this coordinate space representation, here we take the analysis up to the two-loop level. This does not merely correspond to rederiving or rephrasing known results for QCD in magnetic fields in an alternative framework. Rather, our analysis goes beyond the literature by (i) analyzing how the nature of the pion-pion interaction in the pressure – repulsive or attractive – is affected by the magnetic field, as well as temperature and pion mass, and (ii) by providing the low-temperature series for the pressure in weak magnetic fields ($|qH| \ll T^2$) in the chiral limit.

In terms of the dressed pions at zero temperature, the low-temperature expansion of the pressure in a magnetic field takes a remarkably simple form. Non-interacting pions yield the well-known T^4 -contribution, while interaction effects enter at order T^6 . In the chiral limit ($M \rightarrow 0$) – irrespective of whether or not the magnetic field is present – the two-loop interaction contribution vanishes. In the case $M \neq 0$, the pion-pion interaction in the pressure is mostly attractive, but may become repulsive at low temperatures as the magnetic field strength grows. In general, sign and magnitude of the interaction depend on the actual values of temperature, magnetic field, and pion masses in a nontrivial way, as we illustrate in various figures.

In the chiral limit, the low-temperature expansion of the pressure in a weak magnetic field H is dominated by terms involving $\epsilon^{3/2}$, $\epsilon^2 \log \epsilon$ and ϵ^2 , where $\epsilon = |qH|/T^2$ is the relevant expansion parameter and q is the electric charge of the pion.

The article is organized as follows. The evaluation of the QCD partition function in a magnetic field up to two-loop order within chiral perturbation theory is presented in Sec. 2. The nature of the pion-pion interaction in the pressure – attractive or repulsive – is analyzed in Sec. 3. We then focus in Sec. 4 on the thermodynamic properties in the chiral limit and provide the weak magnetic field expansion of the pressure to arbitrary order in $\epsilon = |qH|/T^2$. Finally, in Sec. 5 we conclude. While details on the two-loop CHPT evaluation are discussed in Appendix A, the rather technical analysis of the pressure in weak magnetic fields in the chiral limit is presented in Appendix B.

2 Chiral Perturbation Theory Evaluation

2.1 Preliminaries

Surveys of chiral perturbation theory have been provided on many occasions (see, e.g., Refs. [63, 64]) – in what follows we only touch upon the very basic elements to set the notation. Throughout the study, we refer to the isospin limit $m_u = m_d$.

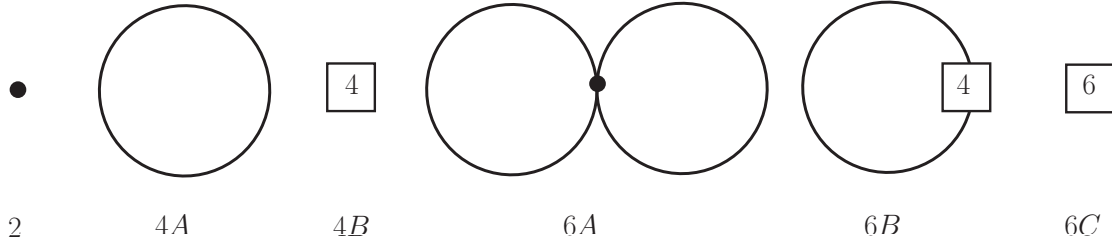


Figure 1: QCD partition function diagrams up to order $p^6 \propto T^6$. The filled circle stands for \mathcal{L}_{eff}^2 , the numbers 4 and 6 in the boxes represent \mathcal{L}_{eff}^4 and \mathcal{L}_{eff}^6 .

The effective pion fields $\pi^i(x)$ appear in the $SU(2)$ matrix $U(x)$,

$$U(x) = \exp(i\tau^i \pi^i(x)/F), \quad i = 1, 2, 3, \quad (2.1)$$

where τ^i are Pauli matrices and F represents the pion decay constant at tree level. The leading piece in the effective Lagrangian is of momentum order p^2 and takes the form

$$\mathcal{L}_{eff}^2 = \frac{1}{4}F^2 \text{Tr} \left[(D_\mu U)^\dagger (D_\mu U) - M^2 (U + U^\dagger) \right]. \quad (2.2)$$

Here M is the pion mass at tree level. The magnetic field H enters via the covariant derivative

$$D_\mu U = \partial_\mu U + i[Q, U]A_\mu^{EM}, \quad (2.3)$$

where Q is the charge matrix of the quarks, $Q = \text{diag}(2/3, -1/3)e$. The gauge field $A_\mu^{EM} = (0, 0, -Hx_1, 0)$ contains the (constant) magnetic field [61].

In the present analysis, we also need higher-order pieces of the effective Lagrangian, namely \mathcal{L}_{eff}^4 and \mathcal{L}_{eff}^6 . The explicit structure is given, e.g., in Refs. [65, 66]. The relevant Feynman diagrams for the partition function up to two-loop order p^6 are shown in Fig. 1. The lines represent thermal propagators which either correspond to the charged pions or the neutral pion. In fact, the dimensionally regularized zero-temperature propagator $\Delta^0(x)$ for the neutral pion in Euclidean space takes the familiar form

$$\Delta^0(x) = (2\pi)^{-d} \int d^d p e^{ipx} (M^2 + p^2)^{-1} = \int_0^\infty d\rho (4\pi\rho)^{-d/2} e^{-\rho M^2 - x^2/4\rho}. \quad (2.4)$$

On the other hand, the dimensionally regularized zero-temperature propagator $\Delta^\pm(x)$ for the charged pions does involve the magnetic field. In Euclidean space, as derived in Ref. [62], it amounts to

$$\Delta^\pm(x) = \frac{|qH|}{(4\pi)^{\frac{d}{2}}} e^{-s_\perp |qH| x_1 x_2 / 2} \int_0^\infty d\rho \frac{\rho^{-\frac{d}{2}+1} e^{-\rho M^2}}{\sinh(|qH|\rho)} \exp \left[-\frac{x_4^2 + x_3^2}{4\rho} - \frac{|qH|(x_1^2 + x_2^2)}{4 \tanh(|qH|\rho)} \right], \quad (2.5)$$

where

$$s_\perp = \text{sign}(qH). \quad (2.6)$$

In either case – for neutral and charged pions – the thermal propagators are obtained by the summing over zero-temperature propagators as

$$G(x) = \sum_{n=-\infty}^{\infty} \Delta(\vec{x}, x_4 + n\beta), \quad \beta = \frac{1}{T}. \quad (2.7)$$

In the evaluation of the partition function diagrams displayed in Fig. 1, as we will see, thermal propagators only have to be considered at the origin $x=0$. It is furthermore advantageous to isolate the zero-temperature pieces Δ^\pm and Δ^0 in the thermal propagators via

$$\begin{aligned} G^\pm(0) &\equiv G_1^\pm = \Delta^\pm(0) + g_1^\pm(M, T, H), \\ G^0(0) &\equiv G_1^0 = \Delta^0(0) + g_1(M, T, 0). \end{aligned} \quad (2.8)$$

The quantities $g_1^\pm(M, T, H)$ and $g_1(M, T, 0)$ are kinematical functions that describe the purely finite-temperature part. They are embedded in the more general class of Bose functions defined by

$$\begin{aligned} g_r^\pm(M, T, H) &= \frac{T^{d-2r-2}}{(4\pi)^{r+1}} |qH| \int_0^\infty d\rho \frac{\rho^{r-\frac{d}{2}}}{\sinh(|qH|\rho/4\pi T^2)} \exp\left(-\frac{M^2}{4\pi T^2}\rho\right) \left[S\left(\frac{1}{\rho}\right) - 1\right], \\ g_r(M, T, 0) &= \frac{T^{d-2r}}{(4\pi)^r} \int_0^\infty d\rho \rho^{r-\frac{d}{2}-1} \exp\left(-\frac{M^2}{4\pi T^2}\rho\right) \left[S\left(\frac{1}{\rho}\right) - 1\right], \\ S(z) &= \sum_{n=-\infty}^{\infty} \exp(-\pi n^2 z), \end{aligned} \quad (2.9)$$

where $S(z)$ is the Jacobi theta function. Note that $g_r(M, T, 0)$ does not involve the magnetic field. In order to facilitate the subsequent analysis, in the Bose functions $g_r^\pm(M, T, H)$ for the charged pions, we extract the $H=0$ part as

$$g_r^\pm(M, T, H) = \tilde{g}_r(M, T, H) + g_r(M, T, 0), \quad (2.10)$$

where solely

$$\begin{aligned} \tilde{g}_r(M, T, H) &= \frac{T^{d-2r-2}}{(4\pi)^{r+1}} |qH| \int_0^\infty d\rho \rho^{r-\frac{d}{2}} \left(\frac{1}{\sinh(|qH|\rho/4\pi T^2)} - \frac{4\pi T^2}{|qH|\rho} \right) \\ &\quad \times \exp\left(-\frac{M^2}{4\pi T^2}\rho\right) \left[S\left(\frac{1}{\rho}\right) - 1\right] \end{aligned} \quad (2.11)$$

contains the magnetic field. These two types of kinematical functions – $\tilde{g}_r(M, T, H)$ and $g_r(M, T, 0)$ – constitute the basic building blocks in our analysis. The decomposition of the thermal propagators into $T=0$ and finite- T pieces then results in

$$\begin{aligned} G_1^\pm &= \Delta^\pm(0) + \tilde{g}_1(M, T, H) + g_1(M, T, 0), \\ G_1^0 &= \Delta^0(0) + g_1(M, T, 0). \end{aligned} \quad (2.12)$$

As a low-energy effective field theory, chiral perturbation theory describes QCD in the regime where quark masses are small, magnetic fields are weak and temperatures are low: the quantities M , H and T ought to be small compared to the QCD scale $\Lambda_{QCD} \approx 1 \text{ GeV}$. While ratios between these parameters in principle can have any value, in the present analysis, the limits $M/T \rightarrow 0$ (chiral limit at fixed temperature) and $|qH| \ll T^2$ (weak magnetic field limit) are of particular interest.

2.2 Free Energy Density up to Order p^6

The one-loop free energy density (order p^4) – in coordinate space representation – has been derived in Ref. [62]. The final renormalized expression reads

$$z_{2+4A+4B} = z_0^{[4]} - \frac{3}{2}g_0(M, T, 0) - \tilde{g}_0(M, T, H). \quad (2.13)$$

The zero-temperature part $z_0^{[4]}$ is¹

$$\begin{aligned} z_0^{[4]} = & -F^2 M^2 + \frac{M^4}{64\pi^2} \left(\bar{l}_3 - 4\bar{h}_1 - \frac{3}{2} \right) + \frac{|qH|^2}{96\pi^2} (\bar{h}_2 - 1) \\ & - \frac{|qH|^2}{16\pi^2} \int_0^\infty d\rho \rho^{-2} \left(\frac{1}{\sinh(\rho)} - \frac{1}{\rho} + \frac{\rho}{6} \right) \exp\left(-\frac{M^2}{|qH|} \rho \right). \end{aligned} \quad (2.14)$$

Modulo factors of $\gamma_3/32\pi^2$, $\delta_1/32\pi^2$, and $\delta_2/32\pi^2$, the quantities \bar{l}_3 , \bar{h}_1 , and \bar{h}_2 represent the running effective coupling constants evaluated at the renormalization scale $\mu = M_\pi$ ($M_\pi \approx 140 \text{ MeV}$) – details can be found, e.g., in Ref. [67].

At the two-loop level (order p^6) the three partition function diagrams 6A–C have to be evaluated – this is done in appendix A. In terms of the tree-level pion mass M , the outcome is

$$\begin{aligned} z_{6A+6B+6C} = & z_0^{[6]} + \frac{3M^2}{8F^2} (g_1)^2 + \frac{M^2}{2F^2} g_1 \tilde{g}_1 \\ & + g_1 \left[-\frac{3\bar{l}_3}{64\pi^2} \frac{M^4}{F^2} + \frac{M^2}{2F^2} K_1 + \frac{\bar{l}_6 - \bar{l}_5}{48\pi^2} \frac{|qH|^2}{F^2} \right] \\ & + \tilde{g}_1 \left[-\frac{\bar{l}_3}{32\pi^2} \frac{M^4}{F^2} + \frac{\bar{l}_6 - \bar{l}_5}{48\pi^2} \frac{|qH|^2}{F^2} \right], \end{aligned} \quad (2.15)$$

where the integral K_1 is defined in Eq. (A.5). Since we are interested in the behavior of the system at finite temperature, the explicit structure of the $T=0$ contribution $z_0^{[6]}$ is not needed here.

¹The third term in the first parenthesis should read $-\frac{3}{2}$. In Ref. [62], Eq. (A7), it was inadvertently cited as -1.

Let us have a closer look at the terms linear in g_1 and \tilde{g}_1 . First notice that the kinematical functions g_1 and \tilde{g}_1 are related to g_0 and \tilde{g}_0 through

$$g_1 = -\frac{\partial g_0}{\partial M^2}, \quad \tilde{g}_1 = -\frac{\partial \tilde{g}_0}{\partial M^2}. \quad (2.16)$$

In presence of a magnetic field, the mass of a charged pion (M_π^\pm) is different from the mass of a neutral pion (M_π^0). In order to determine these masses, we express the kinematical functions g_0 and \tilde{g}_0 in terms of M_π^\pm and M_π^0 – instead of M . Since only the charged pions are tied to \tilde{g}_r^2 , we can write

$$\tilde{g}_0(M_\pi^\pm, T, H) = \tilde{g}_0(M, T, H) - \tilde{g}_1(M, T, H) \tilde{\epsilon}_1, \quad (2.17)$$

where $\tilde{\epsilon}_1$ measures the mass square difference

$$\tilde{\epsilon}_1 = (M_\pi^\pm)^2 - M^2. \quad (2.18)$$

Comparing with the third line of Eq. (2.15), we identify $\tilde{\epsilon}_1$ as

$$\tilde{\epsilon}_1 = \frac{\bar{l}_6 - \bar{l}_5}{48\pi^2} \frac{|qH|^2}{F^2} - \frac{\bar{l}_3}{32\pi^2} \frac{M^4}{F^2}. \quad (2.19)$$

As for g_r – where all three pions are involved according to Eq. (2.12) – we must distinguish between the respective pieces: for the charged pions we write

$$g_0(M_\pi^\pm, T, 0) = g_0(M, T, 0) - g_1(M, T, 0) \tilde{\epsilon}_1, \quad (2.20)$$

while for the neutral pion we have

$$g_0(M_\pi^0, T, 0) = g_0(M, T, 0) - g_1(M, T, 0) \epsilon_1. \quad (2.21)$$

The quantity ϵ_1 measures the mass square difference

$$\epsilon_1 = (M_\pi^0)^2 - M^2, \quad (2.22)$$

and can be identified as

$$\epsilon_1 = -\frac{\bar{l}_3}{32\pi^2} \frac{M^4}{F^2} + \frac{M^2}{F^2} K_1. \quad (2.23)$$

As a result, we can read off how the pion masses are affected by the magnetic field,

$$\begin{aligned} (M_\pi^\pm)^2 &= M_\pi^2 + \frac{\bar{l}_6 - \bar{l}_5}{48\pi^2} \frac{|qH|^2}{F^2}, \\ (M_\pi^0)^2 &= M_\pi^2 + \frac{M^2}{F^2} K_1. \end{aligned} \quad (2.24)$$

Note that M_π is the pion mass in zero magnetic field given by

$$M_\pi^2 = M^2 - \frac{\bar{l}_3}{32\pi^2} \frac{M^4}{F^2} + \mathcal{O}(M^6). \quad (2.25)$$

²See Eq. (2.12).

The mass relations (2.24) indeed coincide with those obtained by Andersen in Ref. [10] – see Eqs. (3.8)-(3.10) – in the zero-temperature limit. It should be pointed out that we consider the pion masses at zero temperature, while in Ref. [10] finite temperature effects are included as well. As it turns out, to have a clear definition of interaction effects in the thermodynamic quantities, we must consider the pion masses at $T=0$, i.e., dress the pions at zero temperature according to Eq. (2.24).

The result for the total two-loop free energy density simplifies considerably if we now express the kinematical functions g_0 and \tilde{g}_0 in the one-loop contribution – Eq. (2.13) – by the masses M_π^\pm and M_π^0 rather than by M . Using Eqs. (2.17), (2.20), and (2.21), we obtain

$$\begin{aligned} z_{tot} = & z_0 - g_0(M_\pi^\pm, T, 0) - \frac{1}{2}g_0(M_\pi^0, T, 0) - \tilde{g}_0(M_\pi^\pm, T, H) \\ & + \frac{M_\pi^2}{2F^2} g_1(M_\pi^\pm, T, 0) g_1(M_\pi^0, T, 0) - \frac{M_\pi^2}{8F^2} \left\{ g_1(M_\pi^0, T, 0) \right\}^2 \\ & + \frac{M_\pi^2}{2F^2} g_1(M_\pi^0, T, 0) \tilde{g}_1(M_\pi^\pm, T, H) + \mathcal{O}(p^8), \end{aligned} \quad (2.26)$$

where z_0 is the zero-temperature piece. The crucial point is that all terms linear in $g_1(M, T, 0)$ and $\tilde{g}_1(M, T, H)$ have been absorbed into mass renormalization: $M^2 \rightarrow (M_\pi^\pm)^2, (M_\pi^0)^2$. In particular, the effect of the pion-pion interaction at finite temperature is solely contained in the terms quadratic in the kinematical functions. It should be noted that the difference between M_π^2 , Eq. (2.25), and the tree-level mass M^2 – at the order we are considering – is irrelevant in the coefficients accompanying the terms quadratic in the kinematical functions, such that it is legitimate write M_π^2 .

While the evaluation of the two-loop free energy density in Refs. [9, 10] is based on a momentum-space representation for the kinematical functions, here we have used an alternative representation based on coordinate space. The advantage is that the latter approach allows for a clear-cut expansion of thermodynamic quantities in the chiral limit as we demonstrate below.

3 Pressure: Nature of Pion-Pion Interaction

We now explore the manifestation of the pion-pion interaction in the pressure which we derive from the two-loop free energy density as

$$P = z_0 - z_{tot}. \quad (3.1)$$

To make temperature powers in the pressure manifest, we replace the Bose functions g_r and \tilde{g}_r by the dimensionless kinematical functions h_r and \tilde{h}_r according to

$$h_0 = \frac{g_0}{T^4}, \quad \tilde{h}_0 = \frac{\tilde{g}_0}{T^4}, \quad h_1 = \frac{g_1}{T^2}, \quad \tilde{h}_1 = \frac{\tilde{g}_1}{T^2}, \quad (3.2)$$

and obtain the low-temperature expansion of the pressure as

$$P = p_1(t, m, m_H) T^4 + p_2(t, m, m_H) T^6 + \mathcal{O}(T^8), \quad (3.3)$$

with coefficients

$$\begin{aligned} p_1(t, m, m_H) &= h_0(M_\pi^\pm, T, 0) + \frac{1}{2}h_0(M_\pi^0, T, 0) + \tilde{h}_0(M_\pi^\pm, T, H) \\ p_2(t, m, m_H) &= -\frac{m^2}{2t^2 F^2} h_1(M_\pi^\pm, T, 0) h_1(M_\pi^0, T, 0) + \frac{m^2}{8t^2 F^2} \left\{ h_1(M_\pi^0, T, 0) \right\}^2 \\ &\quad - \frac{m^2}{2t^2 F^2} h_1(M_\pi^0, T, 0) \tilde{h}_1(M_\pi^\pm, T, H). \end{aligned} \quad (3.4)$$

The dimensionless parameters t, m , and m_H ,

$$t = \frac{T}{4\pi F}, \quad m = \frac{M_\pi}{4\pi F}, \quad m_H = \frac{\sqrt{|qH|}}{4\pi F}, \quad (3.5)$$

measure temperature, pion mass M_π , Eq.(2.25), and magnetic field strength with respect to the scale $4\pi F \approx \Lambda_{QCD}$, i.e., with respect to the renormalization group invariant scale $\Lambda_{QCD} \approx 1\text{GeV}$. In the domain where chiral perturbation theory operates, these parameters are small: more concretely, in the plots below, we will restrict ourselves to the parameter region $t, m, m_H \lesssim 0.3$. For the pion masses we use $M_\pi = 140\text{ MeV}$ and, following Ref. [68], for the pion decay constant we get $F = 85.6\text{ MeV}$. Finally, according to Ref. [65], for the combination of NLO low-energy constants as it appears in the charged pion masses, we take $\bar{l}_6 - \bar{l}_5 = 2.64$.

The T^4 -contribution in the low-temperature series for the pressure corresponds to the non-interacting pion gas, while the pion-pion interaction emerges at order T^6 . Recall that the Bose functions h_0 and h_1 do not involve the magnetic field: the effect of the magnetic field is embedded in the Bose functions \tilde{h}_0 and \tilde{h}_1 . In the chiral limit ($M \rightarrow 0$), the coefficient $p_2(t, m, m_H)$ tends to zero: the pion-pion interaction only starts manifesting itself at the three-loop level, as is well-known for the case $H = 0$ (see, e.g., Ref. [67]). However, for $M \neq 0$, the interaction term is present and – depending on the actual values of the parameters t, m and m_H – the pion-pion interaction in the pressure may result attractive or repulsive, as we now illustrate.

To get a more quantitative picture, let us consider the dimensionless ratio

$$\xi_P(t, m, m_H) = \frac{p_2(t, m, m_H) T^2}{p_1(t, m, m_H)} \quad (3.6)$$

that measures magnitude and sign of the pion-pion interaction relative to the non-interacting pion gas contribution. In Fig. 2 we depict this ratio for the four temperatures $t = \{0.05, 0.1, 0.15, 0.2\}$, or equivalently, $T = \{53.8, 108, 161, 215\}\text{ MeV}$.

In the limit $M \rightarrow 0$, irrespective of absence or presence of the magnetic field, the two-loop interaction contribution vanishes. In the other limit $H \rightarrow 0$, the interaction in the pressure always is attractive, irrespective of the actual values of the

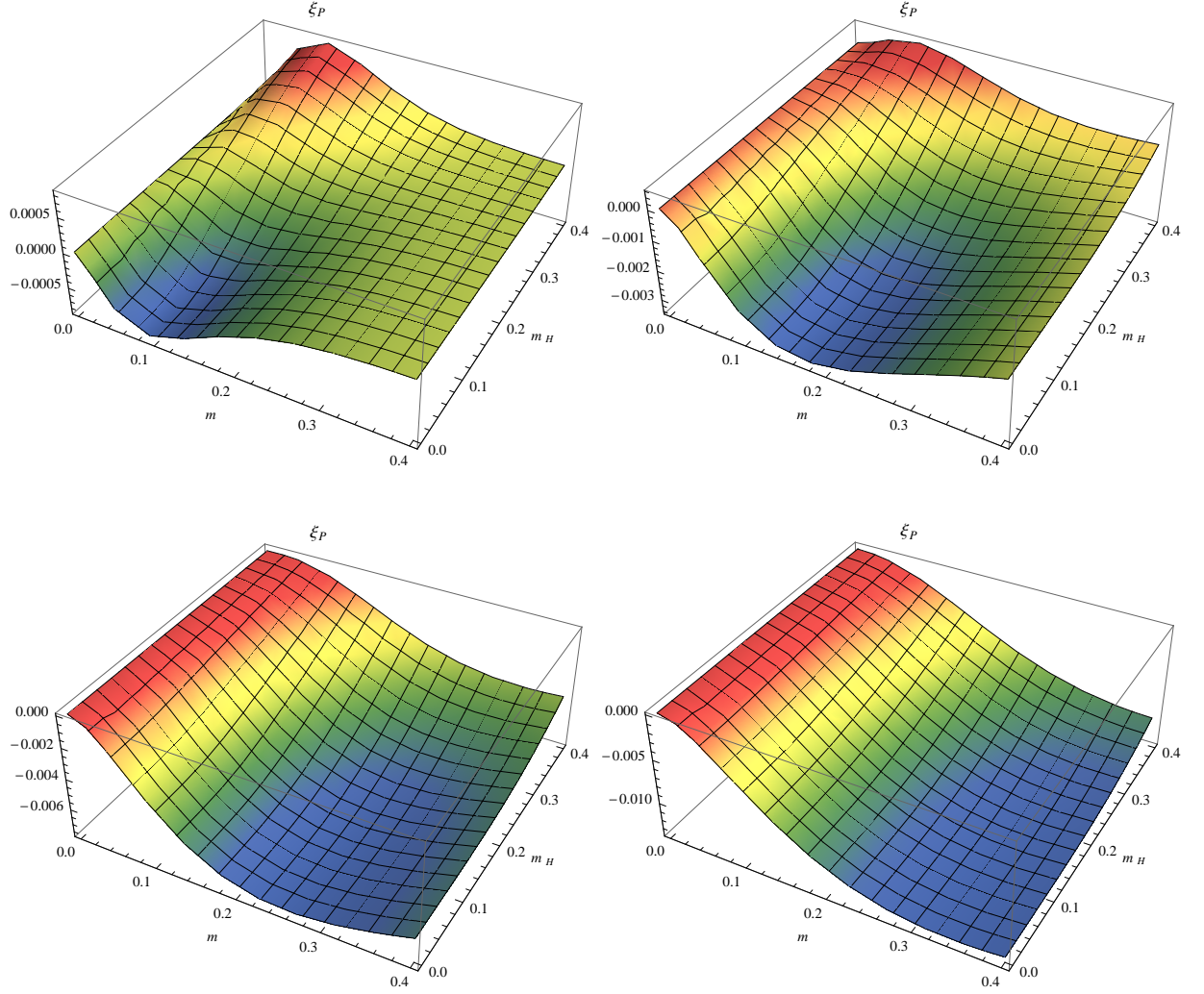


Figure 2: [Color online] Magnitude and sign of the pion-pion interaction in the pressure measured by $\xi_P(t, m, m_H)$ – Eq. (3.6) – for the temperatures $T = 53.8 \text{ MeV}, 108 \text{ MeV}$ (upper panel) and $T = 161 \text{ MeV}, 215 \text{ MeV}$ (lower panel).

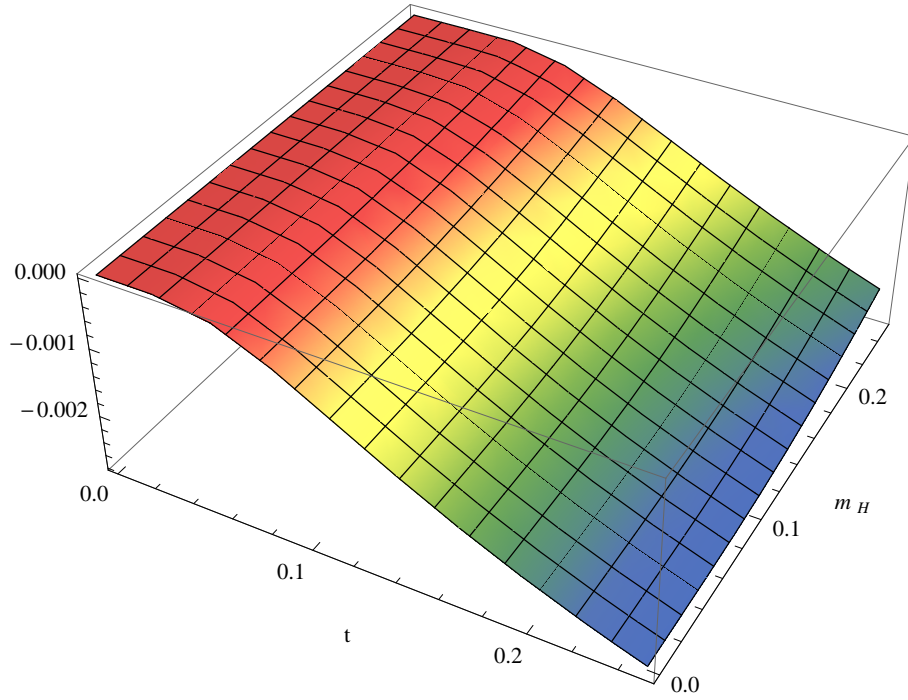


Figure 3: [Color online] Magnitude and sign of the pion-pion interaction in the QCD pressure as a function of temperature (t) and magnetic field strength (m_H) – measured by $p_2(t, m, m_H) T^2$ – at the physical value $M_\pi = 140 \text{ MeV}$ of the pion masses.

(nonzero) pion masses and temperature. When the magnetic field is switched on, the attractive pion-pion interaction becomes weaker, but only at low temperatures and stronger magnetic fields does the pion-pion interaction become repulsive. Overall, the interaction in the pressure is quite small, at most around one percent compared to the leading free Bose gas contribution.

The case of interest corresponding to the physical value of the pion masses – $M_\pi = 140 \text{ MeV}$, i.e., $m = 0.130^3$ – is depicted in Fig. 3 where we plot the dimensionless two-loop contribution $p_2(t, m, m_H) T^2$ as a function of temperature and magnetic field strength. As the figure suggests, the interaction is purely attractive in the parameter domain $t, m_H \leq 0.25$. As the strength of the magnetic field grows, the attractive interaction gradually becomes weaker. Note that the maximal values for the parameters t and m_H correspond to $T \approx 269 \text{ MeV}$ and $\sqrt{|qH|} \approx 269 \text{ MeV}$, respectively. In other words, we are already in a region where temperature and magnetic field strength are no longer small compared to the underlying scale Λ_{QCD} and the low-temperature expansion starts to break down.

³Note that we refer to the isospin limit where all three pions have the same mass (in the absence of the magnetic field).

4 Pressure in Weak Magnetic Fields in the Chiral Limit

The objective of Ref. [62] was to provide the correct low-temperature series for the one-loop quark condensate in weak magnetic fields in the chiral limit. The corresponding analysis involved the kinematical function \tilde{g}_1 . Regarding the pressure, the one-loop contribution involves the kinematical function \tilde{g}_0 . In appendix B, we derive the expansion of this function in weak magnetic fields in the chiral limit, following analogous strategies as for \tilde{g}_1 . Based on these results, we now discuss the structure of the weak magnetic field expansion of the pressure in the chiral limit up to two-loop order which is new to the best of our knowledge.

In the chiral limit, as stated previously, the pion-pion interaction in the pressure starts showing up only at three-loop order which is beyond the scope of our investigation. The low-temperature series for the pressure in the chiral limit is hence fixed by the Bose contribution of order T^4 that contains the kinematical function \tilde{g}_0 . With the weak magnetic field expansion for \tilde{g}_0 , Eq. (B.27), the low-temperature series for the pressure in weak magnetic fields and in the chiral limit takes the form

$$\begin{aligned}
 P = & \frac{\pi^2}{30} T^4 + \left\{ -\frac{|I_{\frac{3}{2}}|}{8\pi^{3/2}} \epsilon^{\frac{3}{2}} - \frac{1}{96\pi^2} \epsilon^2 \log \epsilon + b_1 \epsilon^2 + \mathcal{O}(\epsilon^4) \right\} T^4 \\
 & - (\tilde{l}_6 - \tilde{l}_5) \left\{ \frac{t^2}{144\pi} \epsilon^2 - \frac{t^2 |I_{\frac{1}{2}}|}{96\pi^{5/2}} \epsilon^{\frac{5}{2}} + \frac{t^2 \log 2}{192\pi^3} \epsilon^3 + \mathcal{O}(\epsilon^4) \right\} T^4 \\
 & + \mathcal{O}(T^8 \log T),
 \end{aligned} \tag{4.1}$$

where the relevant expansion parameter $\epsilon \ll 1$ is

$$\epsilon = \frac{|qH|}{T^2}. \tag{4.2}$$

The quantities

$$I_{\frac{3}{2}} \approx -0.610499, \quad b_1 \approx 0.00581159, \quad I_{\frac{1}{2}} \approx -1.516256, \tag{4.3}$$

are defined in Eqs. (B.23), (B.24), and (B.8), respectively.

The series is dominated by a term involving the half-integer power $(|qH|/T^2)^{3/2}$, a logarithmic term $|qH|^2/T^4 \log |qH|/T^2$ and two terms quadratic in the magnetic field. If no magnetic field is present, the series reduces to the well-known pion gas contribution

$$P(H=0) = \frac{\pi^2}{30} T^4 + \mathcal{O}(T^8 \log T). \tag{4.4}$$

5 Conclusions

Within chiral perturbation theory – based on a coordinate space representation for the thermal propagators – we have analyzed the impact of the magnetic field on the partition function up to the two-loop level. Using the dressed pion masses at zero temperature, we have shown that the pion-pion interaction in the pressure may be attractive, repulsive, or zero. The respective sign of the two-loop interaction contribution is controlled by the strength of the magnetic field, as well as temperature and pion mass. In the chiral limit, the interaction is purely attractive at two-loop order, and gradually becomes weaker as the strength of the magnetic field increases.

We then have provided the low-temperature expansion of the pressure in weak magnetic fields in the chiral limit. The dominant terms in the series are proportional to $(|qH|/T^2)^{3/2}$, $|qH^2|/T^4 \log |qH|/T^2$ and $|qH^2|/T^4$.

The question arises whether three-loop corrections in the thermodynamic quantities – i.e., order- p^8 effects – are large compared to the two-loop results discussed here. While the corresponding three-loop analysis referring to zero magnetic field has been provided in Refs. [67, 69], a three-loop analysis for QCD in presence of a magnetic field, based on chiral perturbation theory, has never been attempted to the best of our knowledge. Work in this direction, relying on the coordinate space representation, is currently in progress.

Acknowledgments

The author thanks G. S. Bali, J. Bijnens and H. Leutwyler for correspondence, as well as R. A. Sáenz and C. Castaño Bernard for illuminating discussions.

A Free Energy Density at Two Loops

In this appendix we derive the order- p^6 contribution to the free energy density, originating from diagrams 6A-C of Fig. 1. The two-loop diagram yields

$$z_{6A} = \frac{M^2}{2F^2} G_1^\pm G_1^0 - \frac{M^2}{8F^2} G_1^0 G_1^0, \quad (\text{A.1})$$

where the thermal propagators G_1^\pm for the charged pions and G_1^0 for the neutral pion are defined in Eq. (2.8). The result for the one-loop graph 6B,

$$z_{6B} = (4l_5 - 2l_6) \frac{|qH|^2}{F^2} G_1^\pm + 2l_3 \frac{M^4}{F^2} G_1^\pm + l_3 \frac{M^4}{F^2} G_1^0, \quad (\text{A.2})$$

involves various NLO effective constants l_i that require renormalization (see below). The explicit structure of the tree-level contribution z_{6C} is not required here, because we are interested in the properties of the system at finite temperature.

In the decomposition of thermal propagators,

$$\begin{aligned} G_1^\pm &= \Delta^\pm(0) + \tilde{g}_1(M, T, H) + g_1(M, T, 0), \\ G_1^0 &= \Delta^0(0) + g_1(M, T, 0), \end{aligned} \quad (\text{A.3})$$

the kinematical functions are finite in the limit $d \rightarrow 4$. The zero-temperature propagators $\Delta^\pm(0)$ and $\Delta^0(0)$, however, become singular and take the form

$$\Delta^\pm(0) = 2M^2\lambda + K_1, \quad \Delta^0(0) = 2M^2\lambda. \quad (\text{A.4})$$

The integral K_1 and the parameter λ are

$$\begin{aligned} K_1(M, H) &= \frac{|qH|^{\frac{d}{2}-1}}{(4\pi)^{\frac{d}{2}}} \int_0^\infty d\rho \rho^{-\frac{d}{2}+1} \exp\left(-\frac{M^2}{|qH|}\rho\right) \left(\frac{1}{\sinh(\rho)} - \frac{1}{\rho}\right), \\ \lambda &= \frac{1}{2} (4\pi)^{-\frac{d}{2}} \Gamma(1 - \frac{1}{2}d) M^{d-4} \\ &= \frac{M^{d-4}}{16\pi^2} \left[\frac{1}{d-4} - \frac{1}{2} \{\ln 4\pi + \Gamma'(1) + 1\} + \mathcal{O}(d-4) \right]. \end{aligned} \quad (\text{A.5})$$

Gathering results, the unrenormalized free energy density at order p^6 amounts to

$$\begin{aligned} z^{[6]} &= z_{6A} + z_{6B} + z_{6C} \\ &= \frac{3M^2}{8F^2} (g_1)^2 + \frac{M^2}{2F^2} g_1 \tilde{g}_1 \\ &\quad + g_1 \left[\frac{3M^4}{2F^2} \lambda + \frac{M^2}{2F^2} K_1 + (4l_5 - 2l_6) \frac{|qH|^2}{F^2} + 3l_3 \frac{M^4}{F^2} \right] \\ &\quad + \tilde{g}_1 \left[\frac{M^4}{F^2} \lambda + (4l_5 - 2l_6) \frac{|qH|^2}{F^2} + 2l_3 \frac{M^4}{F^2} \right] \\ &\quad + \frac{3M^6}{2F^2} \lambda^2 + \frac{M^4}{F^2} K_1 \lambda + (8l_5 - 4l_6) \frac{|qH|^2 M^2}{F^2} \lambda + (4l_5 - 2l_6) \frac{|qH|^2}{F^2} K_1 \\ &\quad + 6l_3 \frac{M^6}{F^2} \lambda + 2l_3 \frac{M^4}{F^2} K_1 + z_{6C}. \end{aligned} \quad (\text{A.6})$$

The first two terms are quadratic in the kinematical functions and are finite as d approaches the physical dimension $d=4$. Considering the terms linear in g_1 and \tilde{g}_1 ,

$$\begin{aligned} g_1 &\left[\frac{3M^4}{2F^2} \lambda + \frac{M^2}{2F^2} K_1 + (4l_5 - 2l_6) \frac{|qH|^2}{F^2} + 3l_3 \frac{M^4}{F^2} \right], \\ \tilde{g}_1 &\left[\frac{M^4}{F^2} \lambda + (4l_5 - 2l_6) \frac{|qH|^2}{F^2} + 2l_3 \frac{M^4}{F^2} \right], \end{aligned} \quad (\text{A.7})$$

using the standard convention for the renormalized NLO effective constants \bar{l}_i ,

$$l_i = \gamma_i \left(\lambda + \frac{\bar{l}_i}{32\pi^2} \right), \quad \gamma_3 = -\frac{1}{2}, \quad \gamma_5 = -\frac{1}{6}, \quad \gamma_6 = -\frac{1}{3}, \quad (\text{A.8})$$

we arrive at

$$\begin{aligned} & +g_1 \left[-\frac{3\bar{l}_3}{64\pi^2} \frac{M^4}{F^2} + \frac{M^2}{2F^2} K_1 + \frac{\bar{l}_6 - \bar{l}_5}{48\pi^2} \frac{|qH|^2}{F^2} \right] \\ & +\tilde{g}_1 \left[-\frac{\bar{l}_3}{32\pi^2} \frac{M^4}{F^2} + \frac{\bar{l}_6 - \bar{l}_5}{48\pi^2} \frac{|qH|^2}{F^2} \right]. \end{aligned} \quad (\text{A.9})$$

Notice that the above expressions are perfectly finite: all divergences in Eq. (A.7) have been canceled. Finally, the zero-temperature divergences contained in $z_{6A} + z_{6B}$ – displayed in the last two lines of Eq. (A.6) – will be canceled by counterterms from the next-to-next-to-leading order Lagrangian \mathcal{L}_{eff}^6 contained in the zero-temperature contribution z_{6C} .

B Kinematical Functions in Weak Magnetic Fields

In this appendix we provide the low-temperature representations for the kinematical functions in weak magnetic fields. From the very beginning we operate in the chiral limit. The relevant functions in the free energy density are

$$g_0(0, T, 0), \quad g_1(0, T, 0), \quad (\text{B.1})$$

that do not involve the magnetic field, and

$$\tilde{g}_0(0, T, H), \quad \tilde{g}_1(0, T, H), \quad (\text{B.2})$$

that do depend on the magnetic field. The low-temperature analysis for the former functions in the chiral limit has been given a long time ago in Ref. [67],

$$g_0(0, T, 0) = \frac{\pi^2}{45} T^4, \quad g_1(0, T, 0) = \frac{1}{12} T^2. \quad (\text{B.3})$$

The latter two functions are defined as

$$\tilde{g}_r(0, T, H) = \frac{|qH|^{\frac{d}{2}-r}}{(4\pi)^{\frac{d}{2}}} \int_0^\infty d\rho \rho^{r-\frac{d}{2}} \left(\frac{1}{\sinh(\rho)} - \frac{1}{\rho} \right) \left[S\left(\frac{|qH|}{4\pi T^2 \rho}\right) - 1 \right], \quad (\text{B.4})$$

with

$$S(z) = \sum_{n=-\infty}^{\infty} \exp(-\pi n^2 z). \quad (\text{B.5})$$

The evaluation of $\tilde{g}_1(0, T, H)$ in weak magnetic fields has been established in Ref. [62] with the result

$$\tilde{g}_1(0, T, H) = - \left\{ \frac{|I_{\frac{1}{2}}|}{8\pi^{3/2}} \sqrt{\epsilon} - \frac{\log 2}{16\pi^2} \epsilon + \frac{\zeta(3)}{384\pi^4} \epsilon^2 - \frac{7\zeta(7)}{98304\pi^8} \epsilon^4 + \mathcal{O}(\epsilon^6) \right\} T^2. \quad (\text{B.6})$$

The expansion parameter ϵ measures the ratio between magnetic field strength and temperature,

$$\epsilon = \frac{|qH|}{T^2}. \quad (\text{B.7})$$

By definition, in the weak magnetic field limit $|qH| \ll T^2$, this parameter is small. The integral $I_{\frac{1}{2}}$ is

$$I_{\frac{1}{2}} = \int_0^\infty d\rho \rho^{-1/2} \left(\frac{1}{\sinh(\rho)} - \frac{1}{\rho} \right) \approx -1.516256. \quad (\text{B.8})$$

What remains to be done is the analogous expansion for $\tilde{g}_0(0, T, H)$. According to Ref. [62], the representation (B.4) can be cast into the form

$$\begin{aligned} \tilde{g}_r(0, T, H) &= \frac{\epsilon}{(4\pi)^{r+1}} T^{d-2r} \int_0^1 d\rho \rho^{-\frac{d}{2}+r} \left(\frac{1}{\sinh(\epsilon\rho/4\pi)} - \frac{4\pi}{\epsilon\rho} \right) \left[S\left(\frac{1}{\rho}\right) - 1 \right] \\ &\quad + \frac{\epsilon}{(4\pi)^{r+1}} T^{d-2r} \left\{ I_A + I_B + I_C \right\}, \end{aligned} \quad (\text{B.9})$$

where the respective integrals are defined as

$$\begin{aligned} I_A &= \int_0^1 d\rho \rho^{\frac{d}{2}-r-\frac{5}{2}} \left(\frac{1}{\sinh(\epsilon/4\pi\rho)} - \frac{4\pi\rho}{\epsilon} \right) \left[S\left(\frac{1}{\rho}\right) - 1 \right], \\ I_B &= \int_0^1 d\rho \rho^{\frac{d}{2}-r-\frac{5}{2}} \left(\frac{1}{\sinh(\epsilon/4\pi\rho)} - \frac{4\pi\rho}{\epsilon} \right), \\ I_C &= - \int_0^1 d\rho \rho^{\frac{d}{2}-r-2} \left(\frac{1}{\sinh(\epsilon/4\pi\rho)} - \frac{4\pi\rho}{\epsilon} \right). \end{aligned} \quad (\text{B.10})$$

For $r=0$ and $d \rightarrow 4$, the integral in the first line of Eq. (B.9), much like the integral I_A , are well-defined. Following Ref. [62], the integral I_B is split up into two terms,

$$\begin{aligned} I_B &= I_{B1} + I_{B2}, \\ I_{B1} &= \frac{\epsilon^{\frac{d}{2}-r-\frac{3}{2}}}{(4\pi)^{\frac{d}{2}-r-\frac{3}{2}}} \int_0^\infty d\rho \rho^{-\frac{d}{2}+r+\frac{1}{2}} \left(\frac{1}{\sinh(\rho)} - \frac{1}{\rho} \right), \\ I_{B2} &= - \int_0^1 d\rho \rho^{-\frac{d}{2}+r+\frac{1}{2}} \left(\frac{1}{\sinh(\epsilon\rho/4\pi)} - \frac{4\pi}{\epsilon\rho} \right). \end{aligned} \quad (\text{B.11})$$

For $r=0$ and $d \rightarrow 4$ we obtain

$$\begin{aligned} I_{B1} &= \frac{\sqrt{\epsilon}}{\sqrt{4\pi}} \int_0^\infty d\rho \rho^{-\frac{3}{2}} \left(\frac{1}{\sinh(\rho)} - \frac{1}{\rho} \right), \\ I_{B2} &= - \int_0^1 d\rho \rho^{-\frac{3}{2}} \left(\frac{1}{\sinh(\epsilon\rho/4\pi)} - \frac{4\pi}{\epsilon\rho} \right). \end{aligned} \quad (\text{B.12})$$

Note that the power $\sqrt{\epsilon}$ in I_{B1} is explicit, whereas ϵ appears in the integrand of I_{B2} , as well as in the integrand in the first line of Eq. (B.9) and in I_A of Eq. (B.10), as argument of the hyperbolic sine function. We thus Taylor expand these pieces into

$$\begin{aligned} \frac{1}{\sinh(\epsilon\rho/4\pi)} - \frac{4\pi}{\epsilon\rho} &= c_1 \rho \epsilon + c_2 \rho^3 \epsilon^3 + c_3 \rho^5 \epsilon^5 + \mathcal{O}(\epsilon^7), \\ \frac{1}{\sinh(\epsilon/4\pi\rho)} - \frac{4\pi\rho}{\epsilon} &= c_1 \rho^{-1} \epsilon + c_2 \rho^{-3} \epsilon^3 + c_3 \rho^{-5} \epsilon^5 + \mathcal{O}(\epsilon^7), \end{aligned} \quad (\text{B.13})$$

such that ϵ -powers in all these integrals become explicit. The first few coefficients c_p in the above series are

$$\begin{aligned} c_1 &= -\frac{1}{24\pi} \approx -1.33 \times 10^{-2}, \\ c_2 &= \frac{7}{23\,040\,\pi^3} \approx 9.80 \times 10^{-6}, \\ c_3 &= -\frac{31}{15\,482\,880\,\pi^5} \approx -6.54 \times 10^{-9}, \\ c_4 &= \frac{127}{9\,909\,043\,200\,\pi^7} \approx 4.24 \times 10^{-12}, \\ c_5 &= -\frac{73}{896\,909\,967\,360\,\pi^9} \approx -2.73 \times 10^{-15}. \end{aligned} \quad (\text{B.14})$$

The last piece in the analysis of $\tilde{g}_0(0, T, H)$ in weak magnetic fields is I_C defined in Eq. (B.10). This integral for $r=0$, however, cannot be processed in the manner outlined in Ref. [62] which indeed worked for the case $r=1$ ⁴. Instead, we decompose the integral I_C

$$I_C = - \int_0^1 d\rho \left(\frac{1}{\sinh(\epsilon/4\pi\rho)} - \frac{4\pi\rho}{\epsilon} \right) \quad (\text{B.15})$$

in an alternative way as

$$\begin{aligned} I_C(N) &= I_{C1}(N) + I_{C2}(N) \\ &= - \int_0^N d\rho \left(\frac{1}{\sinh(\epsilon/4\pi\rho)} - \frac{4\pi\rho}{\epsilon} \right) + \int_1^N d\rho \left(\frac{1}{\sinh(\epsilon/4\pi\rho)} - \frac{4\pi\rho}{\epsilon} \right), \end{aligned} \quad (\text{B.16})$$

⁴In the decomposition $I_C = I_{C1} + I_{C2}$, Eq. (A15) of Ref. [62], both expressions I_{C1} and I_{C2} are singular if $r=0$ and $d \rightarrow 4$.

where $N \gg 1$. Redefining integration variables, we obtain

$$\begin{aligned} I_{C1}(N) &= -\frac{\epsilon}{4\pi} \int_{\epsilon/4\pi N}^1 d\rho \rho^{-2} \left(\frac{1}{\sinh(\rho)} - \frac{1}{\rho} \right) - \frac{\epsilon}{4\pi} \int_1^\infty d\rho \rho^{-2} \left(\frac{1}{\sinh(\rho)} - \frac{1}{\rho} \right), \\ I_{C2}(N) &= \frac{\epsilon}{4\pi} \int_{\epsilon/4\pi N}^{\epsilon/4\pi} d\rho \rho^{-2} \left(\frac{1}{\sinh(\rho)} - \frac{1}{\rho} \right). \end{aligned} \quad (\text{B.17})$$

The N -dependence cancels in the sum $I_{C1}(N) + I_{C2}(N)$, and we are left with

$$I_C = \frac{\epsilon}{4\pi} \int_1^{\epsilon/4\pi} d\rho \rho^{-2} \left(\frac{1}{\sinh(\rho)} - \frac{1}{\rho} \right) - \frac{\epsilon}{4\pi} \int_1^\infty d\rho \rho^{-2} \left(\frac{1}{\sinh(\rho)} - \frac{1}{\rho} \right). \quad (\text{B.18})$$

In the second contribution, the power ϵ is explicit. In the first contribution where ϵ appears in the upper integration limit, we Taylor expand the integrand, and then integrate term by term. The final result for I_C can be cast into the form

$$I_C = -\frac{\epsilon}{24\pi} \log\left(\frac{\epsilon}{4\pi}\right) + \frac{\hat{J} - \hat{I}}{4\pi} \epsilon - \sum_{n=2}^{\infty} \frac{2^{2n-1} - 1}{(n-1)(2n)!} \frac{B_{2n}}{(4\pi)^{2n-1}} \epsilon^{2n-1}, \quad (\text{B.19})$$

where the B_{2n} are Bernoulli numbers and the quantities \hat{J} and \hat{I} are defined as

$$\begin{aligned} \hat{J} &= \sum_{n=2}^{\infty} \frac{2^{2n-1} - 1}{(n-1)(2n)!} B_{2n} \approx -0.00924219, \\ \hat{I} &= \int_1^\infty d\rho \rho^{-2} \left(\frac{1}{\sinh(\rho)} - \frac{1}{\rho} \right) \approx -0.179499. \end{aligned} \quad (\text{B.20})$$

Note that the structure of the ϵ -expansion of I_C is now manifest.

Collecting individual contributions, after some algebra, and with the help of the identity

$$\frac{2}{\pi^{\frac{z}{2}}} \Gamma\left(\frac{z}{2}\right) \zeta(z) = \int_0^\infty d\rho \rho^{\frac{z}{2}-1} \left[S(\rho) - 1 \right], \quad (\text{B.21})$$

the expansion of the kinematical function $\tilde{g}_0(0, T, H)$ in weak magnetic fields and in the chiral limit takes the form

$$\begin{aligned} \tilde{g}_0(0, T, H) &= \left\{ -\frac{|I_{\frac{3}{2}}|}{8\pi^{3/2}} \epsilon^{\frac{3}{2}} - \frac{1}{96\pi^2} \epsilon^2 \log \epsilon + b_1 \epsilon^2 \right. \\ &\quad \left. + b_2 \epsilon^4 + b_3 \epsilon^6 + b_4 \epsilon^8 + \mathcal{O}(\epsilon^{10}) \right\} T^4, \end{aligned} \quad (\text{B.22})$$

where

$$I_{\frac{3}{2}} = \int_0^\infty d\rho \rho^{-\frac{3}{2}} \left(\frac{1}{\sinh(\rho)} - \frac{1}{\rho} \right) \approx -0.610499. \quad (\text{B.23})$$

The coefficient b_1 is

$$b_1 = \frac{6(\hat{J} - \hat{I}) - \tilde{I} + \log 4\pi}{96\pi^2} \approx 0.00581159, \quad (\text{B.24})$$

with

$$\tilde{I} = \int_0^1 d\rho \left(\rho^{-1} + \rho^{-\frac{3}{2}} \right) \left[S\left(\frac{1}{\rho}\right) - 1 \right] - \int_0^1 d\rho \rho^{-\frac{1}{2}}, \quad (\text{B.25})$$

while the coefficients b_p ($p \geq 2$) are

$$b_p = -\frac{2(2^{2p-1} - 1)}{(4\pi)^{2p}(2p)!} \left\{ \frac{2\Gamma(2p - \frac{3}{2})\zeta(4p - 3)}{\pi^{2p-\frac{3}{2}}} + \frac{1}{1-p} \right\} B_{2p}, \quad p \geq 2. \quad (\text{B.26})$$

The numerical values of the first five coefficients b_p ($p \geq 2$) are given in Table 1.

p	b_p
2	$- 6.56867042287 \times 10^{-7}$
3	$1.90033315207 \times 10^{-10}$
4	$1.55270844266 \times 10^{-15}$
5	$- 3.08314759762 \times 10^{-16}$
6	$1.87712447343 \times 10^{-18}$

Table 1: The first five coefficients b_p defined by Eq. (B.26).

More explicitly, the series can be written as

$$\begin{aligned} \tilde{g}_0(0, T, H) = & \left\{ -\frac{|I_{\frac{3}{2}}|}{8\pi^{3/2}}\epsilon^{\frac{3}{2}} - \frac{1}{96\pi^2}\epsilon^2 \log \epsilon + \frac{6(\hat{J} - \hat{I}) - \tilde{I} + \log 4\pi}{96\pi^2}\epsilon^2 \right. \\ & - \frac{7(2\pi^2 - 3\zeta(5))}{184320\pi^6}\epsilon^4 + \frac{31(4\pi^4 - 105\zeta(9))}{495452160\pi^{10}}\epsilon^6 \\ & \left. - \frac{127(32\pi^6 - 31185\zeta(13))}{3805072588800\pi^{14}}\epsilon^8 + \mathcal{O}(\epsilon^{10}) \right\} T^4. \end{aligned} \quad (\text{B.27})$$

To check convergence properties of the above series for $\tilde{g}_0(0, T, H)$ in the weak magnetic field limit $|qH| \ll T^2$, let us compare the first few terms in the ϵ -expansion with the exact result Eq. (B.4). The first column in Table 2 displays the exact result, while the second column just takes into account the leading term in the series (B.27) proportional to $\epsilon^{3/2}$. The third column furthermore incorporates the $\epsilon^2 \log \epsilon$ -contribution and the fourth column finally extends up to the ϵ^2 -term. One observes that a very good approximation is achieved by just including the first three terms: the series (B.27) converges quite rapidly.

Finally it should be noted that the order T^4 -contribution in the pressure, i.e., the coefficient p_1 in Eq. (3.4),

$$p_1(t, m, m_H) = h_0(M_\pi^\pm, T, 0) + \frac{1}{2}h_0(M_\pi^0, T, 0) + \tilde{h}_0(M_\pi^\pm, T, H), \quad (\text{B.28})$$

ϵ	\tilde{g}_0/T^4	$\mathcal{O}(\epsilon^{3/2})$	$\mathcal{O}(\epsilon^2 \log \epsilon)$	$\mathcal{O}(\epsilon^2)$
0.1	-3.50963233726 -4	-4.33381291264 -4	-4.09079140529 -4	-3.50963246014 -4
0.05	-1.30789993783 -4	-1.53223424946 -4	-1.45318968180 -4	-1.30789994551 -4
0.01	-1.26375177959 -5	-1.37047197570 -5	-1.32186767423 -5	-1.26375177971 -5
0.005	-4.56026045635 -6	-4.84535013722 -6	-4.70555019271 -6	-4.56026045643 -6
0.001	-4.20279056592 -7	-4.33381291264 -7	-4.26090646044 -7	-4.20279056592 -7
0.0005	-1.49764974370 -7	-1.53223424946 -7	-1.51217871733 -7	-1.49764974370 -7
0.0001	-1.35493952595 -8	-1.37047197570 -8	-1.36075111541 -8	-1.35493952595 -8

Table 2: Exact result and leading terms in the series (B.27) for the kinematical function \tilde{g}_0 in the limit $|qH| \ll T^2$. We use the notation where $-3.50963233726 - 4$ stands for $-3.50963233726 \times 10^{-4}$, etc.

contains the kinematical functions $h_0(M_\pi^\pm, T, 0)$ and $\tilde{h}_0(M_\pi^\pm, T, H)$ which, in the chiral limit, reduce to

$$h_0(M_H, T, 0), \quad \tilde{h}_0(M_H, T, H), \quad (\text{B.29})$$

with

$$(M_H)^2 = \frac{\bar{l}_6 - \bar{l}_5}{48\pi^2} \frac{q^2 H^2}{F^2}. \quad (\text{B.30})$$

In the weak magnetic field limit, the kinematical function $h_0(M_H, T, 0)$ hence takes the form

$$h_0(M_H, T, 0) = h_0(0, T, 0) - \alpha \epsilon^2 h_1(0, T, 0) + \frac{\alpha^2 \epsilon^4}{2} h_2(0, T, 0) + \mathcal{O}(\epsilon^6), \quad (\text{B.31})$$

where

$$\alpha = \frac{\bar{l}_6 - \bar{l}_5}{12\pi} t^2, \quad \epsilon = \frac{|qH|}{T^2}, \quad t = \frac{T}{4\pi F}. \quad (\text{B.32})$$

Analogously, in the weak magnetic field limit, the kinematical function $\tilde{h}_0(M_H, T, H)$ amounts to

$$\tilde{h}_0(M_H, T, H) = \tilde{h}_0(0, T, H) - \alpha \epsilon^2 \tilde{h}_1(0, T, H) + \frac{\alpha^2 \epsilon^4}{2} \tilde{h}_2(0, T, H) + \mathcal{O}(\epsilon^6). \quad (\text{B.33})$$

We hence have additional terms in the weak magnetic field expansion of the pressure in the chiral limit, which contain the NLO low-energy constants \bar{l}_5 and \bar{l}_6 .

References

- [1] I. A. Shushpanov and A. V. Smilga, Phys. Lett. B **402**, 351 (1997).
- [2] N. O. Agasian, Phys. Lett. B **488**, 39 (2000).
- [3] N. O. Agasian, Phys. At. Nucl. **64**, 554 (2001).

- [4] N. O. Agasian and I. A. Shushpanov, JHEP **10**, 006 (2001).
- [5] T. D. Cohen, D. A. McGady, and E. S. Werbos, Phys. Rev. C **76**, 055201 (2007).
- [6] N. O. Agasian, Phys. At. Nucl. **71**, 1967 (2008).
- [7] N. O. Agasian and S. M. Fedorov, Phys. Lett. B **663**, 445 (2008).
- [8] N. O. Agasian, Phys. At. Nucl. **72**, 339 (2009).
- [9] J. O. Andersen, Phys. Rev. D **86**, 025020 (2012).
- [10] J. O. Andersen, JHEP **10**, 005 (2012).
- [11] T. Brauner and S. V. Kadam, JHEP **11**, 103 (2017).
- [12] M. A. Andreichikov and Y. A. Simonov, Eur. Phys. J. C **78**, 902 (2018).
- [13] M. D’Elia, S. Mukherjee, and F. Sanfilippo, Phys. Rev. D **82**, 051501 (2010).
- [14] M. D’Elia and F. Negro, Phys. Rev. D **83**, 114028 (2011).
- [15] G. S. Bali, F. Bruckmann, G. Endrödi, Z. Fodor, S. D. Katz, S. Krieg, A. Schäfer, and K. K. Szabó, JHEP **02**, 044 (2012).
- [16] V. V. Braguta, P. V. Buividovich, T. Kalaydzhyan, S. V. Kuznetsov, and M. I. Polikarpov, Phys. At. Nucl. **75**, 488 (2012).
- [17] G. S. Bali, F. Bruckmann, G. Endrödi, Z. Fodor, S. D. Katz, and A. Schäfer, Phys. Rev. D **86**, 071502 (2012).
- [18] G. S. Bali, F. Bruckmann, M. Constantinou, M. Costa, G. Endrödi, Z. Fodor, S. D. Katz, H. Panagopoulos, and A. Schäfer, Phys. Rev. D **86**, 094512 (2012).
- [19] G. S. Bali, F. Bruckmann, G. Endrödi, F. Gruber, and A. Schäfer, JHEP **04**, 130 (2013).
- [20] V. G. Bornyakov, P. V. Buividovich, N. Cundy, O. A. Kochetkov, and A. Schäfer, Phys. Rev. D **90**, 034501 (2014).
- [21] G. S. Bali, F. Bruckmann, G. Endrödi, S. D. Katz, and A. Schäfer, JHEP **08**, 177 (2014).
- [22] C. Bonati, M. D’Elia, M. Mariti, F. Negro and F. Sanfilippo, Phys. Rev. D **89**, 054506 (2014).
- [23] E.-M. Ilgenfritz, M. Müller-Preussker, B. Petersson, and A. Schreiber, Phys. Rev. D **89**, 054512 (2014).
- [24] M. D’Elia, F. Manigrasso, F. Negro, and F. Sanfilippo, Phys. Rev. D **98**, 054509 (2018).

- [25] G. Endrödi, M. Giordano, S. D. Katz, T. C. Kovács, and F. Pittler, JHEP **07**, 007 (2019).
- [26] R. Gatto and M. Ruggieri, Phys. Rev. D **83**, 034016 (2011).
- [27] A. Amador and J. O. Andersen, Phys. Rev. D **88**, 025016 (2013).
- [28] M. Ferreira, P. Costa, D. P. Menezes, C. Providencia, and N. N. Scoccola, Phys. Rev. D **89**, 016002 (2014).
- [29] M. Ferreira, P. Costa, O. Lourenco, T. Frederico, and C. Providencia, Phys. Rev. D **89**, 116011 (2014).
- [30] M. Ferreira, P. Costa, and C. Providencia, Phys. Rev. D **90**, 016012 (2014).
- [31] E. J. Ferrer, V. de la Incera, I. Portillo, and M. Quiroz, Phys. Rev. D **89**, 085034 (2014).
- [32] M. Ruggieri, Z. Y. Lu, and G. X. Peng, Phys. Rev. D **94**, 116003 (2016).
- [33] R. Zhang, W. Fu, and Y. Liu, Eur. Phys. J. C **76**, 307 (2016).
- [34] T. D. Cohen and E. S. Werbos, Phys. Rev. C **80**, 015203 (2009).
- [35] A. J. Mizher, M. N. Chernodub, and E. S. Fraga, Phys. Rev. D **82**, 105016 (2010).
- [36] S. Nam and C.-W. Kao, Phys. Rev. D **87**, 114003 (2013).
- [37] M. Frasca and M. Ruggieri, Phys. Rev. D **83**, 094024 (2011).
- [38] E. S. Fraga and L. F. Palhares, Phys. Rev. D **86**, 016008 (2012).
- [39] F. Bruckmann, G. Endrödi, and T. G. Kovács, JHEP **04**, 112 (2013).
- [40] G. Endrödi, JHEP **04**, 023 (2013).
- [41] V. D. Orlovsky and Y. A. Simonov, JHEP **09**, 136 (2013).
- [42] J.-P. Blaizot, E. S. Fraga, and L. F. Palhares, Phys. Lett. B **722**, 167 (2013).
- [43] M. Ruggieri, M. Tachibana, and V. Greco, JHEP **07**, 165 (2013).
- [44] G. S. Bali, F. Bruckmann, G. Endrödi, and A. Schäfer, Phys. Rev. Lett. **112**, 042301 (2014).
- [45] G. Colucci, E. S. Fraga, and A. Sedrakian, Phys. Lett. B **728**, 19 (2014).
- [46] V. D. Orlovsky and Y. A. Simonov, Phys. Rev. D **89**, 074034 (2014).
- [47] V. D. Orlovsky and Y. A. Simonov, Phys. Rev. D **89**, 054012 (2014).
- [48] A. Haber, F. Preis, and A. Schmitt, Phys. Rev. D **90**, 125036 (2014).

- [49] N. Mueller and J. M. Pawlowski, Phys. Rev. D **91**, 116010 (2015).
- [50] V. D. Orlovsky and Y. A. Simonov, Int. J. Mod. Phys. A **30**, 1550060 (2015).
- [51] Y. A. Simonov and V. D. Orlovsky, JETP Letters **101**, 423 (2015).
- [52] K. Kamikado and T. Kanazawa, JHEP **01**, 129 (2015).
- [53] L.-G. Pang, G. Endrödi, and H. Petersen, Phys. Rev. C **93**, 044919 (2016).
- [54] A. N. Tawfik, A. M. Diab, N. Ezzelarab, and A. G. Shalaby, Adv. High Energy Phys. **2016**, 1381479 (2016).
- [55] A. Bandyopadhyay, N. Haque and M. G. Mustafa, Phys. Rev. D **100**, 034031 (2019).
- [56] S. Rath and B. K. Patra, JHEP **12**, 098 (2017).
- [57] M. A. Andreichikov and Y. A. Simonov, Eur. Phys. J. C **78**, 420 (2018).
- [58] F. L. Braghin, Eur. Phys. J. A **54**, 45 (2018).
- [59] S. Rath and B. K. Patra, Eur. Phys. J. A **55**, 220 (2019).
- [60] B. Karmakar, R. Ghosh, A. Bandyopadhyay, N. Haque, and M. G. Mustafa, Phys. Rev. D **99**, 094002 (2019).
- [61] J. O. Andersen, W. R. Naylor, and A. Tranberg, Rev. Mod. Phys. **88**, 025001 (2016).
- [62] C. P. Hofmann, Phys. Rev. D **99**, 014030 (2019).
- [63] H. Leutwyler, in *Hadron Physics 94 – Topics on the Structure and Interaction of Hadronic Systems*, edited by V. E. Herscovitz, C. A. Z. Vasconcellos and E. Ferreira (World Scientific, Singapore, 1995), p. 1.
- [64] S. Scherer, Adv. Nucl. Phys. **27**, 277 (2003).
- [65] J. Gasser and H. Leutwyler, Ann. Phys. (N.Y.) **158**, 142 (1984).
- [66] J. Bijnens, G. Colangelo, and G. Ecker, Ann. Phys. **280**, 100 (2000).
- [67] P. Gerber and H. Leutwyler, Nucl. Phys. B **321**, 387 (1989).
- [68] S. Aoki et al., Eur. Phys. J. C **80**, 113 (2020).
- [69] C. P. Hofmann, Nucl. Phys. B **916**, 254 (2017).